Lumped Hysteretic Model for Subsurface Stormflow Developed Using Downward Approach

John Ewen

and

Stephen J. Birkinshaw

University of Newcastle upon Tyne

School of Civil Engineering and Geosciences

Newcastle upon Tyne

NE1 7RU

KEY WORDS downward modelling approach; subsurface stormflow; hysteresis; rainfall-runoff modelling; lumped modelling; catchment-scale modelling

Abstract

The terms "downward" and “upward” (synonymous with “top-down” and “bottom-up”, respectively) are sometimes used when describing methods for developing hydrological models. A downward approach is used here to develop a lumped catchment-scale model for subsurface stormflow at the 0.94 km^2 Slapton Wood catchment. During the development, as few assumptions as possible are made about the behaviour of subsurface stormflow at the catchment scale, and no assumptions are made about its behaviour at smaller scales. (In an upward approach, in contrast, the modelling would be based on assumptions about, and data for, the behaviour at smaller scales, such as the hillslope, plot, and point scales.) The model has a single store with a relatively simple relationship between discharge and storage, based on equations describing hysteretic patterns seen in a graph of discharge against storage. Double-peaked hydrographs have been observed at the catchment outlet. Rainfall on the channel and infiltration-excess and saturation-excess runoff gives a rapid response, and shallow subsurface stormflow gives a delayed response. Hydrographs are successfully simulated for the large delayed responses observed in 1971-80 and 1989-91, then a lumped model for the rapid response is coupled to the lumped hysteretic model and some double-peaked hydrographs simulated. A physical interpretation is developed for the lumped hysteretic model, making use of information on patterns of perched saturation observed in 1982 on a hillslope at the Slapton Wood catchment. Downward and upward approaches are complementary, and the most robust way to develop and improve lumped catchment models is to iterate between downward and upward steps. Possible next steps are described.

Introduction

The Slapton Wood catchment, Devon, UK, (Figure 1) is a small research catchment, 0.94 km^2, with mixed land use, steep slopes, a stream, some dry valleys, and soils that are mainly freely-draining acid brown soils with a clay-loam texture (Burt and Heathwaite, 1996, Trudgill, 1983). When the catchment is wet, there are sometimes double-peaked responses in the outlet discharge hydrograph (right-hand hydrograph in Figure 2). Rainfall on the channel and infiltration-excess and saturation-excess runoff give the rapid response, and shallow subsurface stormflow gives the delayed response (Burt and Heathwaite, 1996). Similar double-peaked responses have been observed in other catchments (e.g. Anderson and Burt, 1978, Chevallier and Planchon, 1993, Hihara and Susuki, 1988). The main evidence supporting the conclusion that the delayed response at Slapton Wood is shallow subsurface stormflow is that there is little visible sign of surface runoff to the stream during the delayed response, and hydrological investigations have discovered shallow perched saturation and subsurface flow (Burt and Heathwaite, 1996, Chappell and Franks, 1996). Also, the nitrate concentration in the stream is highest during delayed responses (Burt and Arkell, 1987), suggesting that the water comes from the shallow subsurface. The perched saturation was observed where a low-permeability layer overlies fractured slate (Chappell and Franks, 1996). When the catchment is dry, there are low flows, thought to be sustained by groundwater discharge from this slate, and short-lived single peaks.

During the period late 1989 to mid 1991, the Institute of Hydrology, UK, carried out intensive fieldwork to collect data to validate the SHETRAN physically-based distributed catchment model (Bathurst, *et al.*, 2004). The fieldwork involved monitoring several variables, including: rainfall, meteorological variables, stream outlet discharge, soil water matric potential, soil water content, and the free water level in dip wells. Various dimensions and properties were also measured for topography, land use, the stream and soils. There were delayed responses in winter 1989-90 that are as large as any seen in the decade 1971-80 (digitised hourly discharge records are available for this decade). Winter 1990-91 had only small delayed responses, but these are comparable in size to the largest seen in some of the less-stormy years in 1971 to 1980. Note that the dip in the hydrograph at 14 March 1990 was caused by a malfunction of the measurement weir, and there is a gap in the rainfall record from 8th December 1990 to 20th December 1990 (Figure 2).

The general picture of subsurface stormflow that emerges from the hydrological investigations is of shallow saturated flow, controlled by gravity and topography, which converges in dry valleys, before discharging to the stream. Based on this picture, and some simple modelling, Burt and Butcher (1985a) concluded that flow convergence on hillslopes is the *"primary topographic mechanism for producing delayed peaks"*. The concepts behind the TOPMODEL topography-based distribution function catchment model are consistent with this picture of subsurface stormflow, and TOPMODEL has been used with the 1989-91 data (Beven and Freer, 2001, Fisher and Beven, 1996). The 1989-91 data have also been used in nitrate modelling using SHETRAN (Birkinshaw and Ewen, 2000, Birkinshaw and Ewen, 2004), as well as in the flow modelling for the validation exercise for which the data were originally collected (Bathurst, *et al.*, 2004).

One thing that is common in all this previous modelling is that the starting point is a fixed model structure, comprising a set of general mathematical equations containing parameters. This structure, quite different from model to model, is assumed to represent the nature of subsurface stormflow (and, similarly, the natures of all the other flows and processes that are represented). To set up the models, some form of calibration or statistical analysis is used to help choose values for the parameters. In the SHETRAN work, for example, particular care had to be taken in calibrating the parameters associated with the hydraulic properties of the perched saturated layer (Birkinshaw and Ewen, 2004).

The purpose in most of this previous modelling was to see if the models can reproduce the hydrograph, and to estimate the predictive uncertainty in simulating the hydrograph, rather than to test the model structures or the way the structures represent subsurface stormflow. However, this modelling has added weight to two of the conclusions drawn from the hydrological investigations, namely: 1) convergence in the dry valleys can affect the delayed response; and 2) the reason the nitrate concentration in the stream is highest during delayed peaks is because the water comes from the shallow subsurface, as subsurface stormflow.

The approach taken here is intrinsically different from that used in previous modelling. It involves using a "downward" (or “top-down”) modelling approach to develop a catchment-scale model for subsurface stormflow at the Slapton Wood catchment. What is important about the downward approach is that the model structure derives from the rainfall, evaporation and discharge data (so is data-based), rather than from any assumptions made about how subsurface stormflow behaves at smaller scales, such as the hillslope, plot, and point scales.

In an “upward” (or “bottom-up”) approach, assumptions are be made about the smaller scale. For example, results from grid-based distributed physically based modelling can be used to derive a lumped large-scale model (Ewen, *et al.*, 1999, Kilsby, *et al.*, 1999).

Method

Ideally, the process of creating and testing a data-based model would simply involve applying tools to the data, one tool in the creation process and another tool in testing, and a physical interpretation would simply reveal itself. Perhaps the nearest to a creation tool is the data-based mechanistic (DBM) method (Young, 2003), where the model structure and parameter set is inferred from the rainfall-runoff data using statistical methods of time series analysis. There are subjective elements in DBM, because it assumes that the model structure belongs to a general class of structures, and this general class has to be defined *a priori*, and the inferred model is accepted only if it is physically reasonable (e.g. if it can somehow be interpreted as a model of physical processes or flows and stores).

Klemes (1983), who coined the terms “downwards” and “upwards”, proposed a more general approach. This involves starting from the forcing and response data and improving the structure by taking a series of steps, upward and downward steps in turn, carefully testing the outcome of each step. His aim was to develop a hierarchy of time and space scales, each with its own conceptualisation, so that it is possible to go up and down in scale in a consistent manner.

The downward approach is a philosophy, rather than a fixed set of tools and rules, so it is capable of wide interpretation and has been used to study several different types of problem (see, for example, Sivapalan, *et al.*, 2003, and the other papers in the special issue this introduces). Here, the interpretation is (deliberately) rather narrow, and the downward approach is applied to developing a model at a single scale, the catchment scale. Basically, the work involves developing a catchment-scale description of subsurface stormflow, while making no assumptions about the behaviour of subsurface stormflow at smaller scales, and making as few assumptions as possible about its behaviour at the catchment scale.

The first assumption is that there is mass balance and the catchment is watertight. Figure 3 is a storage/discharge plot. The storage values were calculated by integrating the mass conservation equation, with an initial value s=0:

$$\frac{ds}{dt} = r - e - q \qquad (1)$$

where e (mm hr^{-1}) is evaporation rate, q (mm hr^{-1}) measured discharge at the catchment outlet, r (mm hr^{-1}) rainfall rate, s (mm) storage, and t (hr) time. The second assumption is that the evaporation rate can be approximated by the potential rate for evaporation from grass, as calculated from meteorological records using the Penman-Monteith equation. This is reasonable when there is significant subsurface stormflow, because the catchment will be wet and the evaporation rate small compared to the rainfall and discharge. It will, though, introduce a cumulative error in the calculation of storage.

Response trajectories can be seen in the storage/discharge plot in Figure 3. Storage increases during storms, and when the storage is increasing (wetting), the direction of travel will be from left to right. The wetting trajectories tend to have shallow slopes if the pre-storm discharge is low (see the trajectory marked “wetting” in Figure 3). The transition from wetting to drying, when the storage stops increasing and begins to fall, is usually associated with a sudden change in slope, from a positive slope to a steep negative slope (e.g. the junction between the trajectories marked “wetting” and “drying” in Figure 3). During drying, the discharge continues to rise for some time until it reaches a maximum (see “delayed peak” in Figure 3), after which it begins to fall. The basic pattern is therefore of anti-clockwise hysteretic loops: wetting (moving upwards on positive slope); transition to drying (change in slope); drying with increasing discharge (moving upwards on steep negative slope); delayed peak; continued drying with reducing discharge (moving downwards on positive slope). Another pattern can be seen in Figure 3. When there are large rapid responses, there can be brief clockwise loops (see “brief clockwise loop” in Figure 3). These are, essentially, just distortions to the wetting trajectories, caused by rapid discharge. They do not correspond to any physical hysteretic behaviour which, say, links rapid discharge to a storage for rapid discharge. If it were possible to eliminate the rapid discharge from the discharge/storage plot, it is likely that the basic pattern of anti-clockwise hysteretic loops would be even more marked than it currently is, especially for the largest events, where the rapid discharge significantly affects the junctions between the wetting and drying trajectories.

There are similarities, from storm to storm, in the shapes of the subsurface stormflow responses, and in the shapes of the recessions. By changing the initial storage and altering the input term in the mass balance equation, it is possible to manipulate the plot so that a general pattern emerges. Figure 4 shows only the drying trajectories (so the direction of travel is always right to left) . Some of the trajectories are quite broken, by short periods of wetting. In the figure, the resulting broken lines should not be confused with the five smooth dashed lines, which are for model trajectories (described later). Figure 4 it is for an initial storage of 20 mm and with r replaced by 0.912r in the integration of Equation 1. Most of the recessions lie on a single curve (the "attractor curve"), and during the largest events the discharge rises to a peak and then falls asymptotically to the attractor curve. In other words, the drying trajectories behave as if they are attracted to the attractor curve.

The general pattern in Figure 4 is far from perfect. For example, the peaks for the second and third largest events look like they should be further to the right. By adjusting the input term, the delayed responses can be made to move right and left, relative to one another. What is suggested by Figure 4, however, is that the main characteristic of subsurface stormflow is that it is attracted to a simple behaviour in which the discharge is a function of storage, and during the attraction the discharge rises to a peak before falling. The third assumption to be made in developing a model for subsurface stormflow is, therefore, that the relationship between storage and discharge can be described using the patterns and values seen in Figure 4. To create the model, these patterns and values must be expressed in equations.

Before the equations are developed, it is worth noting that there are systematic variations in Figure 4 that suggest that the catchment discharge is affected by processes other than subsurface stormflow. For example, the factor 0.912, found by manual trial and error, is probably related to groundwater recharge, in that the "missing" 8.8% of rainfall probably ends up as deep groundwater (this percentage is clearly quite sensitive to errors in the calculation of the factor). Also, the way that some of the drying trajectories run parallel to the attractor curve at storages less than 40 mm can probably be partly explained by the effects of other storage processes. This point will be returned to later.

The attractor curve, fitted by manual trial and error, is:

$$q' = (s'/b)^c \qquad (2)$$

where b=98 mm, c=1.6, and the dash signifies attractor curve. Moore (1997) fitted this equation to shallow subsurface streamflow recessions for a 0.17 km^2 forested catchment in British Columbia, Canada. He used two different objective functions when calibrating the equation. One function gave a value for c of 1.85, and the other 2.13. These, and the value for Slapton Wood (1.6), are quite close to the mean value, 2.04, found by Wittenberg (1999) in a general study of groundwater recessions using data from over 80 gauging stations in Germany. He found values for c lying in a range from less than 1 to greater than 10.

During subsurface stormflow, the drying trajectories on the storage/discharge plot tend to start with a negative slope and are asymptotic to the attractor curve, so end with a positive slope. In between these extremes, the slope appears to vary linearly with the horizontal distance from the attractor curve. Say the current storage and discharge are s and q. It is as if the storage is being attracted to a value $s' = bq^{1/c}$, which is the value of storage where the line starting at point (s,q), drawn parallel to the storage axis, cuts the attractor curve. At this cutting point, the slope of the attractor curve is cq/s'. The horizontal distance is s-s', so a suitable equation for the slope of the trajectory is:

$$\frac{dq}{ds} = \frac{cq}{s'} - \beta(s - s')f \qquad (3)$$

where β is a constant, and f is a function (discussed below). For the largest delayed response in Figure 4, $\beta = 0.002$ mm^{-1} hr^{-1} (assuming f=1). The drying trajectories tend to be flatter at lower values of s', and the function f accounts for this. For the model trajectories plotted in Figure 4, and for all the model trajectories and simulated hydrographs described below, it is assumed that $\beta = 0.002$ mm^{-1} hr^{-1} and f=s'/b (testing will show whether or not these are good choices).

The questions that arise are: 1) how can this model be tested; and 2) if it is correct, what does it say about subsurface stormflow? Ideally, the testing should be able to use the data for 1971-80, as well as for 1989-90, so must rely only on the observed discharge records, because hourly rainfall records are not available for 1971-80. The model, as it stands, describes only the storage-discharge relationship for delayed responses, but it can be used to derive a model for the discharge-time relationship, so that delayed hydrographs can be simulated.

The simulation model will comprise a mass conservation equation, plus a dynamic equation for the discharge hysteresis (i.e. an equation for dq_d/dt , where q_d is the delayed discharge). The mass conservation equation is:

$$\frac{ds}{dt} = i - q_d \qquad (4)$$

where i=r-e is the net input. The important feature of the discharge equation is that, when i=0, the discharge must follow the model trajectories given by Equations 2 and 3. By the chain rule, $dq_d/dt=(dq_d/ds)(ds/dt)$, and $ds/dt=-q_d$ when i=0, so:

$$\frac{dq_d}{dt} = -\left[\frac{cq_d}{s'} - \beta(s - s')f\right]q_d \qquad (5)$$

The lumped hysteretic model for simulating hydrographs therefore comprises Equations 4 and 5, which are a well-behaved coupled pair of initial ordinary differential equations (ODEs).

For any given value of peak delayed discharge, the lumped hysteretic model gives a unique delayed hydrograph: the "signature" hydrograph. Signature hydrographs were calculated by integrating both forwards and backwards in time from the delayed peak, assuming i=0, using a 4th order Runge-Kutta algorithm (Press, *et al.*, 1992). The initial conditions for the integration are s_p, the storage at peak, and q_p, the delayed peak discharge. Given q_p, then $s_p=s'_p+cq_p/(\beta s'_p f)$, which was derived after noting that $dq_d/dt=0$ at the peak.

As well as being used to calculate signature hydrographs, the lumped hysteretic model can be used as a general-purpose simulation model, to simulate the hydrograph over extended periods (e.g. weeks or months during the winter). In reality, there will be other storages and flows that the model neglects (or simply lumps in with subsurface stormflow storage and flow), such as groundwater discharge from the fractured slate. This could lead to a sensitivity problem, associated with the trajectory slope dq_d/ds being steep and negative at the start of large delayed responses, causing any small errors in the calculation of storage to result in large errors in the calculation of discharge. This sensitivity problem is examined later.

The most significant flow that is neglected by the lumped hysteretic model is rapid runoff from the surface. A downward approach is used below to develop a model for this, which is then coupled to the lumped hysteretic model so that double-peaked hydrographs can be simulated.

The main feature of the rapid response is that it is associated with rainfall and with large values of dq/dt. This suggests that the most robust way to develop a dynamic equation for the rapid response is to create an equation that describes the patterns seen in a plot of dq/dt against rainfall. In Figure 5, dq/dt is plotted against r^2 for the observed discharge and rainfall in winter 1989-90. There are clockwise loops in the figure, and the largest loop corresponds to the large brief clockwise loop at the top right hand corner in Figure 3. The model for the rapid response is:

$$\frac{dq_r}{dt} = 0.5(i_r - q_r) \qquad (6)$$

where q_r (mm hr^{-1}) is the rapid discharge. The form of the input term ($i_r=0.006r^2s'/b$) and the value 0.5 (hr^{-1}) were guessed, based on noting that the rapid response is dependent on rainfall and wetness and lasts for only a couple of hours, and the factor 0.006 (hr mm^{-1}) was found by trial and error. The general pattern of slopes and loops is reasonably well represented by the model (Figure 5), and this is probably as much as can be expected using this approach. Whether or not this model is adequate for simulating rapid responses can be judged later when the results from simulations of combined rapid and delayed responses are compared against the observed discharge. For the combined simulations, the three coupled ODEs, Equations 4-6, were integrated using the Runge-Kutta algorithm. The appropriate input term in Equation 4 is then $i=r-e-i_r$, for mass conservation

Results

In Figure 6, signature trajectories are plotted on the same graph as the three largest subsurface stormflow responses for winter 1989-90 ($q_p=0.792$ mm hr^{-1} on 21st Dec.; 0.964 on 3rd Feb.; and 0.783 on 15th Feb.); the main response for winter 1990-91 (0.391 on 20th Mar.); and the two main responses for the decade 1971-80 (0.729 on 21st Feb. 1978; and 0.823 on 11th Feb. 1979). Burt and Heathwaite (1996) show a hydrograph for 27th Jan. 1984, but there is rainfall during the subsurface stormflow response, so the observed hydrograph is flatter than the signature hydrograph.

The most robust way to test the model is to try and disprove it, by searching for observed delayed hydrographs that do not agree with the corresponding signature hydrograph. The hydrographs for all the significant delayed responses in the 1971-80 record were therefore extracted, using an automatic procedure, and are plotted in Figure 7. To be classed as a significant response, the peak discharge had to be greater than 0.3 mm hr^{-1} and the average discharge had to rise for three consecutive 7-hour periods and then fall for five consecutive 7-hour periods. This selection procedure is independent of the model. It automatically rejects rapid responses, and also rejects most of the delayed responses that have rapid fluctuations caused by rainfall. In total, 21 hydrographs were extracted. Only two of these differ markedly from their corresponding signature hydrographs. One hydrograph peaks at around 0.6 mm hr^{-1} (on 30 Nov. 1976), and falls rapidly to below 0.2 mm hr^{-1}. To make this hydrograph easier to see in Figure 7, it is drawn using a thick line. There was 4.5 mm of rainfall on the day of the peak, and 48.8 mm on the previous day. What marks this hydrograph as different from the rest, apart from the rapid fall, is that it starts from a very low level (0.026 mm hr^{-1} at 59 hours prior to peak). It is therefore for large rainfall on a very dry catchment. The other hydrograph peaks at around 0.3 mm hr^{-1} (30th Jan. 1975). This is low, so this hydrograph is much less important. There was 10.2 mm of rainfall on the day of the peak, and a total of 38.9 mm on the previous four days.

Figure 8 demonstrates the sensitivity problem. For all three simulated hydrographs, the initial discharge is assumed equal to the observed discharge, but each has a different initial storage: s-s' = 0, 10, and 20 mm, where s' is calculated from the initial discharge using Equation 2. This same approach to creating initial conditions is used in all the simulations below. Although in Figure 8 the effect of the initial storage decays with time, suggesting that the model is robust against errors in the initial conditions, what the simulations show is that even a small error in the simulated storage at the beginning of a delayed response can give a significant error in the simulated peak delayed discharge.

Figure 9 shows the simulated discharge for the whole period of subsurface stormflow in winter 1989-90. The three simulations converge within 100 hours, and the three dashed lines merge into a thin solid line. Figure 10 shows the delayed response for 20th Mar. 1991, which was included in Figure 6. The peak discharge is low, only 0.391 mm hr^{-1}. The recession continues for a few months after the end of the simulation period, presumably sustained by groundwater discharge. It is clear from all these simulation results that the model is reasonably good at simulating large delayed responses, but less good at simulating small delayed responses.

Physical Interpretation

The lumped hysteretic model was developed based solely on the patterns seen in the storage/discharge plot. As far as possible, the model does not depend on any physical interpretations or conceptual notions, other than those covered by the three assumptions that were noted during the derivation. A model structure with a more conventional structure is developed below. It is entirely consistent with the lumped hysteretic model.

Although the lumped hysteretic model has only one store, it has two state variables: the storage, s, and the attractive storage, s'. Alternatively, the state variables can be said to be the attractive storage, s', and the "excess storage", s-s'. One possible explanation why there is attraction towards the attractor curve is that, as the subsurface stormflow develops, the discharge increasingly becomes controlled by the subsurface hydraulics and flow geometry in the immediate region of the stream, rather than by the flow (transit) towards the stream. The attractive storage can therefore be associated with one store in a conventional lumped model, and the response of this store will be controlled by the attractor curve. The excess storage will then be associated with a second store (Figure 11), and there will be transit, T, between them. The two-store model is a lumped model for the catchment, so this transit applies at the macroscale, and is an aggregation of local flows, as controlled by local water surface slopes, water depths, and by the hydraulic properties of the porous media and land drains (if there are any). Similarly, the input, I, to the attractive store (Figure 11) is an aggregation of the rapid infiltration of rainwater to the volume of water that constitutes the attractive storage.

There are some similarities between this two-store cascade structure and the three-store cascade structure used for modelling the subsurface stormflow in the steep-sided 0.038 km^2 Maimai M8 catchment, New Zealand (Seibert and McDonnell, 2002). This has a hillslope store, supplying water to a hollow store, which in turn supplies water to a riparian store.

Moore (1997) also proposed a two-store model, and observed that it fitted his recession data (in calibration) much more accurately than any of the one-store models he considered. This work was mentioned earlier, where values for c were quoted for Equation 2. Moore’s models, though, were not validated.

If the two-store model is to be entirely consistent with the lumped hysteretic model, then $q'=q_d$, where q' is the discharge from the attractive store and q_d the delayed discharge for the lumped hysteretic model. An equation for the transit, T, can then be derived as follows. Applying the chain rule:

$$\frac{dq_d}{dt} = \frac{dq'}{ds'}\frac{ds'}{dt} \qquad (7)$$

where the term on the left hand side is given by Equation 5, the first factor on the right hand side by Equation 2, and the final factor by the following mass balance equation for the attractive store:

$$\frac{ds'}{dt} = I + T - q' \qquad (8)$$

This gives:

$$T = -I + \beta s'(s - s')f / c \qquad (9)$$

For the simplest possible model structure, I=0, which means that there is no rapid infiltration of rainwater to the volume of water that constitutes the attractive storage. The remaining term in the transit equation is non-linear, as it depends on the product of s', the attractive storage, and s-s', the excess storages (as well as depending on the function f). This dependence on the attractive storage is slightly curious. For the Maimai M8 model, for example, the hillslope and hollow stores release water at rates depending on their storage, but not depending on the storages in the stores that receive the water.

It is possible that the curious form of the transit equation arises simply because the physical interpretation is wrong. For example, perhaps the stores should be assumed stacked one above the other, and T interpreted as the percolation rate from the upper (unsaturated) to the lower (saturated) store. The physical interpretation would then be that the percolation rate depends on the storage in both the unsaturated and saturated stores. This interpretation is entirely reasonable, but it will not be investigated further.

Returning to the analysis of the two-store cascade structure, the question that has arisen is: why are the local flows towards the stream (apparently) controlled by the attractive storage (i.e. the storage further downslope)? Measurements of the depth of saturation above the soil-bedrock interface were reported by Burt and Butcher (1985b) for Eastergrounds Hollow (0.014 ha) in the Slapton Wood catchment during two double-peaked responses in March 1982. There is a spring at the base of the hollow, and the area of saturation feeding the spring expands and contracts in response to the net effect of rainfall, evaporation and drainage. It seems reasonable to assume a connection between the saturated area feeding the spring and the attractive store. The measurements also show that an area of saturation develops on an interfluve plateau. This is initially separate from the area feeding the spring, but as both areas expand in response to rainfall they finally join up (around the time of the delayed peak). The two areas then shrink, in response to evaporation and discharge, until they separate. It seems reasonable to assume a connection between this area of saturation on the plateau and the excess store. The degree of hydraulic connection (and hence transit) between the two areas would be at its maximum when both areas are large, and would be small, or zero, if either area is small. This could be the physical explanation for the form of the transit equation. It must be remembered that the area of Eastergrounds Hollow is only 1.5% of the area of the Slapton Wood catchment, and it is not known what is happening in the other 98.5% during this time. There is, though, a remarkable resemblance in shape between the double-peaked hydrograph measured below the spring (Figure 5 in Burt and Butcher, 1985b) and that shown here for the catchment outlet (Figure 2).

The fact that the areas of saturation become disconnected as a result of drying might also explain why some of the drying trajectories run parallel to the attractor curve at storages less than 40 mm in Figure 4. The storage in Figure 4 is the total storage, but if the excess storage has ceased to drain to the stream, the trajectory will depend only on the attractive storage. This means that the trajectory will tend to have the same shape as the attractor curve, but will be displaced to the right by an amount equal to the excess storage.

Returning to the sensitivity problem discussed earlier, the physical interpretation is simply that there is sensitivity to how much water is in the excess store. This suggests that, for robust modelling, there may be some advantage in using the two-store model, because the excess storage will then have its own mass balance calculations, which will help to isolate the errors in the calculation of the excess storage from the (larger?) errors in the calculation of the total storage.

Future Work

It is interesting to consider what the next steps would be in developing and testing the model. The hysteretic model is reasonably good at simulating large delayed responses, but less good at simulating small delayed responses. Two possible methods for improving the modelling of small delayed responses are: 1) Continue with the downward approach, and investigate the hydrographs for small delayed responses. 2) Use knowledge of the small-scale pattern of saturation at Eastergrounds Hollow, and perhaps also the measurements for the discharge from the spring, to improve the transit equation. This could use a model for the hollow, perhaps a distributed physically-based model.

If the second method above is used, this would mark a transition in the way that the model is being developed and tested. Up to this point, a pure downward approach has been used, but now an upward approach is to be used. Somehow, simulation results from the hollow model have to be used to alter the lumped hysteretic model so that it gives better simulations of small delayed responses. In other words, the aspects of the lumped models behaviour related to small delayed responses have to emulate the corresponding behaviours shown by the hollow model. This type of emulation is the basis for the Upscaled Physically-based model (UP model, Ewen, 1997), as used by Ewen et al. (1999) and Kilsby et al. (Kilsby, *et al.*, 1999), so the techniques used in UP could be used here.

For small events, the field evidence shows that the two saturated areas do not join up (Burt and Butcher, 1985b). The outcome from the hollow modelling might therefore be (to give a concrete example) that the saturated areas remain unconnected until the saturated area connected to the spring reaches some given size. The only change this would require to the lumped hysteretic model would be that the transit, T, would be set to zero if the attractive storage is below some threshold value. A first estimate for the threshold value could be obtained by calibrating the lumped hysteretic model against the hollow model (with suitable scaling, because the hollow covers only 1.5% of the catchment).

Conclusions

A “downward” approach has been used to develop a lumped hysteretic model for subsurface stormflow in the Slapton Wood catchment. This has a single store with a relatively simple hysteretic relationship between storage and discharge. Only three physical assumptions were made in the development of the lumped hysteretic model: 1) There is mass balance and the catchment is watertight. 2) The evaporation rate can be approximated by the potential rate for evaporation from grass, as calculated from meteorological records using the Penman-Monteith equation. Note that the model is applied only when the catchment is wet. 3) The main patterns and values seen in the storage/discharge plot in Figure 4 (which applies at the catchment scale) are characteristic of subsurface stormflow. The model is therefore based on direct evidence of the physical behaviour of subsurface stormflow at the catchment scale, and no assumptions were made about the physical behaviour at smaller scales.

The lumped hysteretic model produces delayed hydrographs which agree with the catchment discharge hydrographs observed during subsurface stormflow in 1971-80 and in winters 1989-90 and 1991-91. A rainfall-runoff model that can simulate the double-peaked hydrographs observed at the Slapton Wood catchment was created by coupling the lumped hysteretic model to a model for the rapid discharge associated with rainfall falling on the channel, and infiltration-excess and saturation-excess runoff.

The lumped hysteretic model was shown to be exactly equivalent to a conventional-looking two-store lumped model (Figure 11), but the equation for the rate of water exchange (transit) between the stores is unconventional. Field data for a hillslope at Slapton Wood (Burt and Butcher, 1985b) suggests that the two stores are associated with perched saturated areas. For this interpretation, the unconventional form of the transit equation arises because of the way that the saturated areas expand and join up during large events, allowing drainage to the stream from saturated areas which are normally hydraulically disconnected from the stream (e.g. interfluve areas), thus generating and sustaining large delayed responses at the catchment outlet.

The lumped hysteretic model could be used as an engineering tool, for predicting discharge. Clearly, though, the maximum scientific gain is obtained only when the model has a physical interpretation, and that interpretation is used to help understanding. The physical interpretation can also be used when further improving the model structure (so can help increase the value of the model as an engineering tool). In considering the next step that could be taken in developing the model, an “upward” approach was therefore proposed, using the available hillslope field data and the model’s physical interpretation which was (partly) based on that data. It was recognised by Klemes (1983) that upward and downward approaches are complementary: "*the most promising route to significant new discoveries in hydrology is to combine the upward and downward search based on the existing facts and knowledge as well as on imagination and intuition, to form testable hypotheses – i.e. to apply the time-honoured scientific method*". Iterating between downward and upward steps when developing and testing a catchment model is, therefore, just the same as iterating between inductive and deductive reasoning when developing and testing a theory.

The main challenges faced in this work were: 1) to stay in control of the assumptions being made (implicitly and explicitly) while developing the model; and 2) working out at every stage how testing should be carried out. If the work on developing the lumped model is to continue with an upward step, the challenge of staying in control of the assumptions will become much harder, because several assumptions will have to be made about physical processes.

Acknowledgements

The 1989-91 data were collected by the Institute of Hydrology as part of a programme of work funded by UK Nirex Ltd. We thank Greg O'Donnell for useful discussions on this work, and Tim Burt and an anonymous reviewer for useful and insightful comments which we put to good use in improving this paper.

References

Anderson M G, Burt T P. 1978. The role of topography in controlling throughflow generation. *Earth Surface Processes and Landforms* **3:** 331-344.

Bathurst J C, Ewen J, Parkin G, O'Connell P E, Cooper J D. 2004. Validation of catchment models for predicting land-use and climate change impacts. 3. Blind validation for internal and outlet responses. *Journal of Hydrology* **287:** 74-94.

Beven K, Freer J. 2001. A dynamic TOPMODEL. *Hydrological Processes* **15:** 1993-2011.

Birkinshaw S J, Ewen J. 2000. Modelling nitrate transport in the Slapton Wood catchment using SHETRAN. *Journal of Hydrology* **230:** 18-33.

Birkinshaw S J, Ewen J. 2004. *SHETRAN Version 5 evaluation modelling for water flow and nitrate transport in the Slapton Wood catchment*. WRSRL/2004_4. Water Resource Systems Research Laboratory, School of Civil Engineering and Geosciences, University of Newcastle. Newcastle upon Tyne. 45pp.

Burt T P, Arkell B P. 1987. Temporal and spatial patterns of nitrate losses from an agricultural catchment. *Soil Use and Management* **3:** 138-142.

Burt T P, Butcher D P. 1985a. On the generation of delayed peaks in stream discharge. *Journal of Hydrology* **78:** 361-378.

Burt T P, Butcher D P. 1985b. Topographic controls of soil moisture distributions. *Journal of Soil Science* **36:** 469-486.

Burt T P, Heathwaite A L. 1996. The hydrology of the Slapton catchments. *Field Studies* **8:** 543-557.

Chappell N A, Franks S W. 1996. Property distributions and flow structure in the Slapton Wood catchment. *Field Studies* **8:** 559-575.

Chevallier P, Planchon O. 1993. Hydrological processes in a small humid savanna basin (Ivory Coast). *Journal of Hydrology* **151:** 173-191.

Ewen J. 1997. 'Blueprint' for the UP modelling system for large scale hydrology. *Hydrology and Earth System Sciences* **1:** 55-69.

Ewen J, Sloan W T, Kilsby C G, O'Connell P E. 1999. UP modelling system for large scale hydrology: deriving large-scale physically-based parameters for the Arkansas-Red River Basin. *Hydrology and Earth System Sciences* **3:** 125-136.

Fisher J, Beven K J. 1996. Modelling of stream flow at Slapton Wood using TOPMODEL within an uncertainty estimation framework. *Field Studies* **8:** 577-584.

Hihara T, Susuki K. 1988. The double peak hydrograph during storm events in a small watershed of the Tama hills, west of Tokyo. *Geographical Review of Japan* **61A:** 804-815.

Kilsby C G, Ewen J, Sloan W T, Burton A, Fallows C S, O'Connell P E. 1999. The UP modelling system for large scale hydrology: simulation of the Arkansas-Red River Basin. *Hydrology and Earth System Sciences* **3:** 137-149.

Klemes V. 1983. Conceptualization and scale in hydrology. *Journal of Hydrology* **65:** 1-23.

Moore R D. 1997. Storage-outflow modelling of streamflow recessions, with application to a shallow-soil forested catchment. *Journal of Hydrology* **198:** 260-270.

Press W H, Teukolsky S A, Vetterling W T, Flannery B P. 1992. *In Numerical Recipes in FORTRAN 77*. Cambridge University Press. Cambridge, UK.

Seibert J, McDonnell J J. 2002. On the dialog between experimentalist and modeler in catchment hydrology: Use of soft data for multicriteria model calibration. *Water Resources Research* **38:** 1241. doi:10.1029/2001WR000978.

Sivapalan M, Bloschl G, Zhang L, Vertessy R. 2003. Downward approach to hydrological prediction. *Hydrological Processes* **17:** 2101-2111.

Trudgill S T. 1983. The natural history of Slapton Ley Nature Reserve. XVI. The soils of Slapton Wood. *Field Studies* **5:** 833-840.

Wittenberg H. 1999. Baseflow recession and recharge as nonlinear storage process. *Hydrological Processes* **13:** 715-726.

Young P. 2003. Top-down and data-based mechanistic modelling of rainfall-flow dynamics at the catchment scale. *Hydrological Processes* **17:** 2195-2217.

Figures

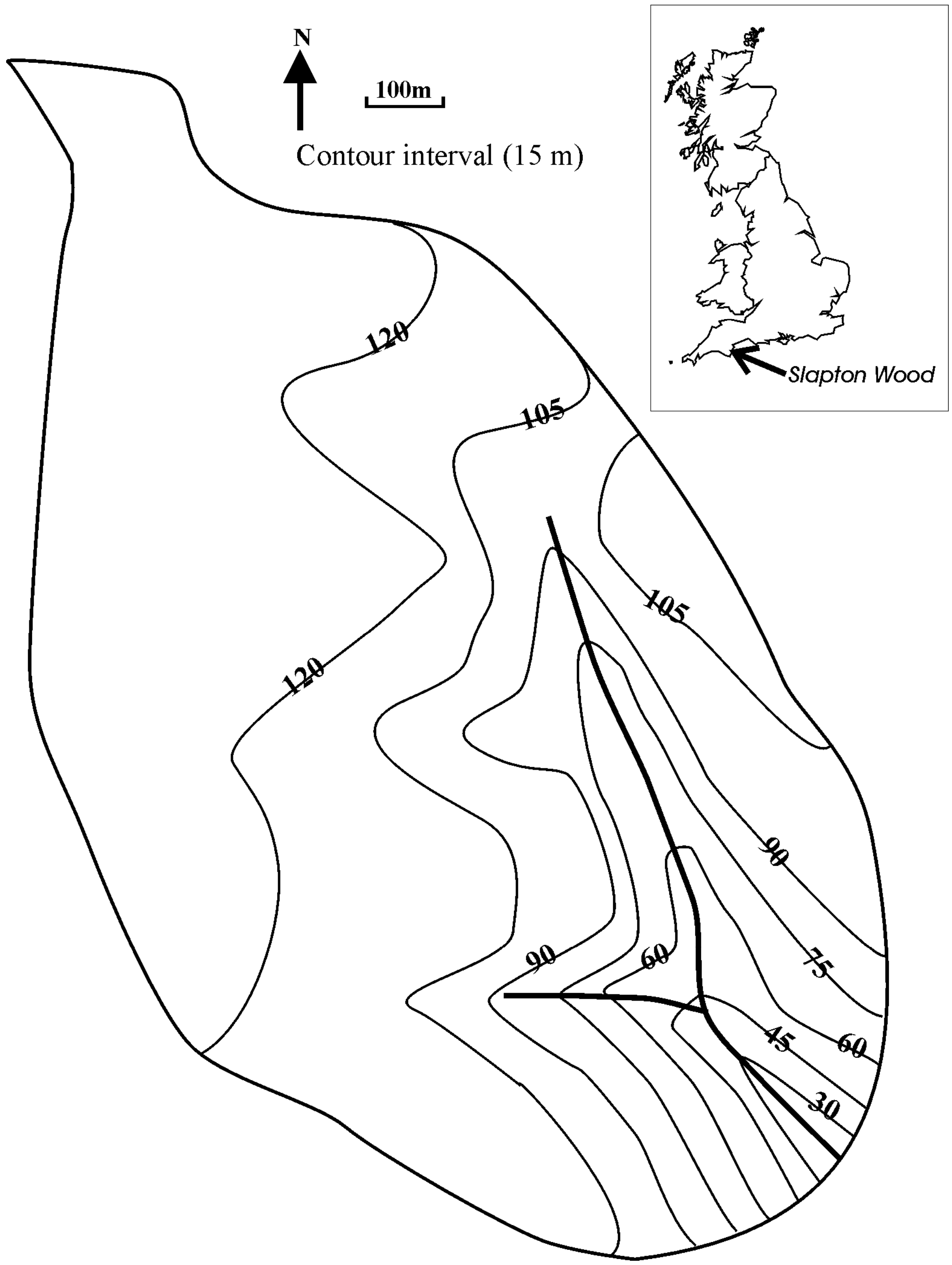

Figure 1 Slapton Wood Catchment.

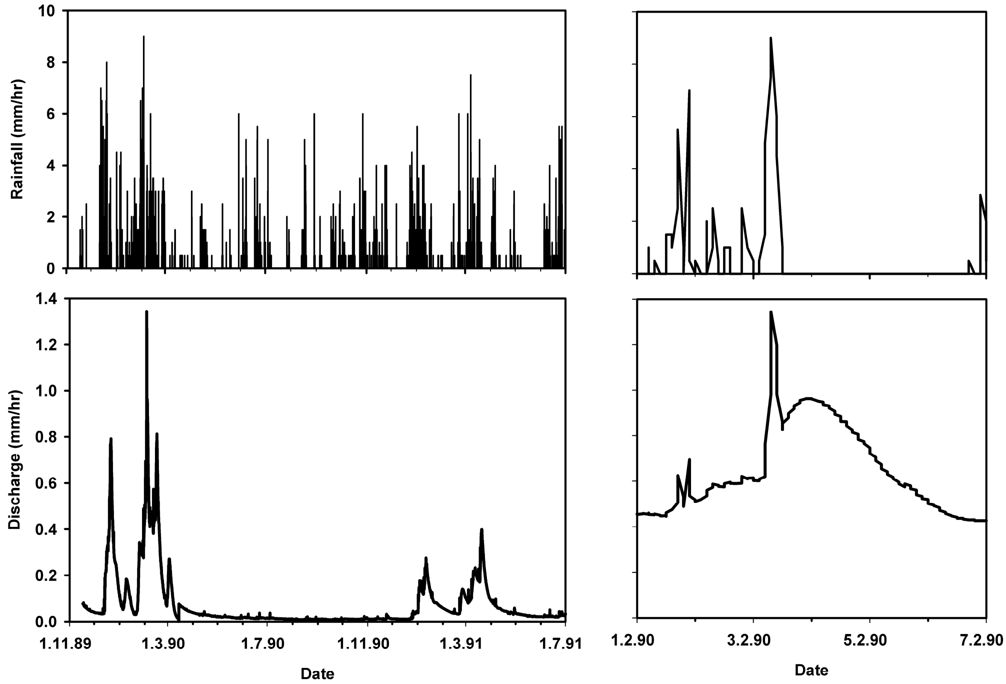

Figure 2 Observed rainfall and discharge, and the largest double peaked response.

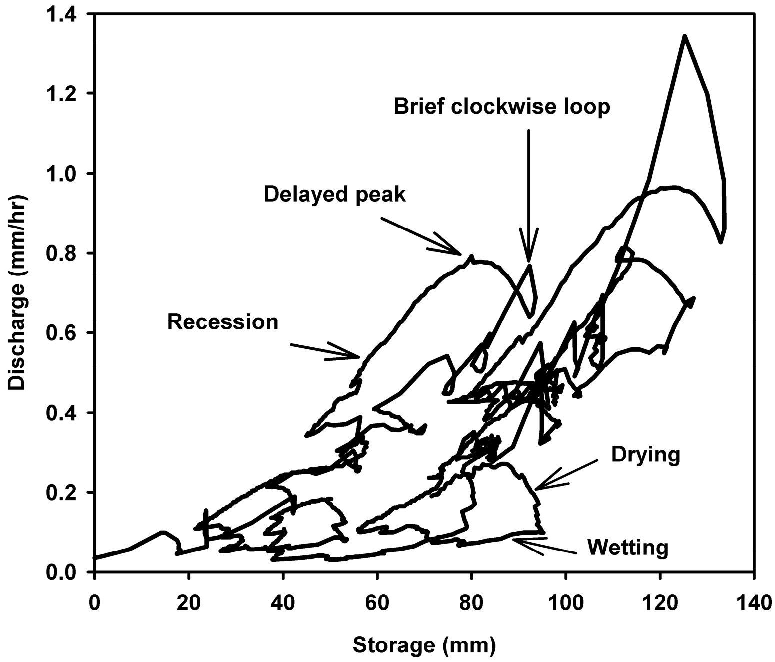

Figure 3 Storage/discharge plot for 13th December 1989 to 4th March 1990, inclusive.

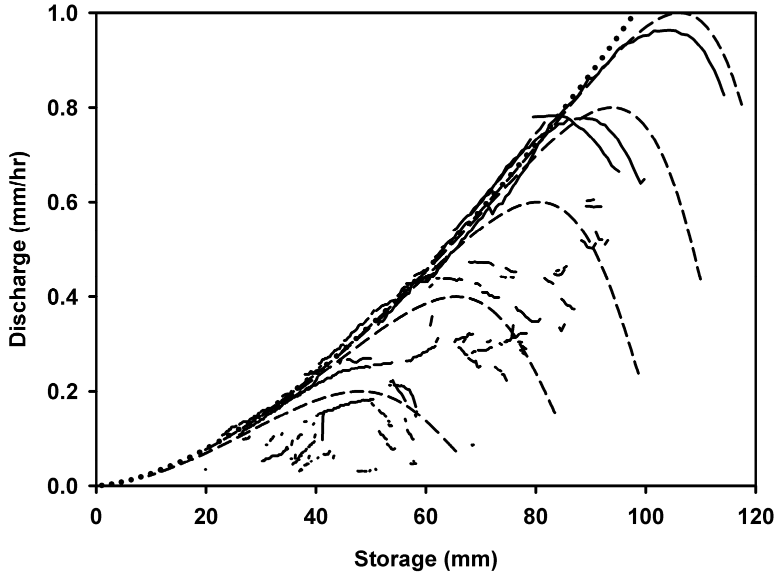

Figure 4 Adjusted drying trajectories (solid lines) for 13th December 1989 to 4th March 1990, inclusive, plus the attractor curve (dots) and signature trajectories (smooth dashed lines) for peak discharges of 0.2, 0.4, 0.6, 0.8 and 1.0 mm hr^{-1}.

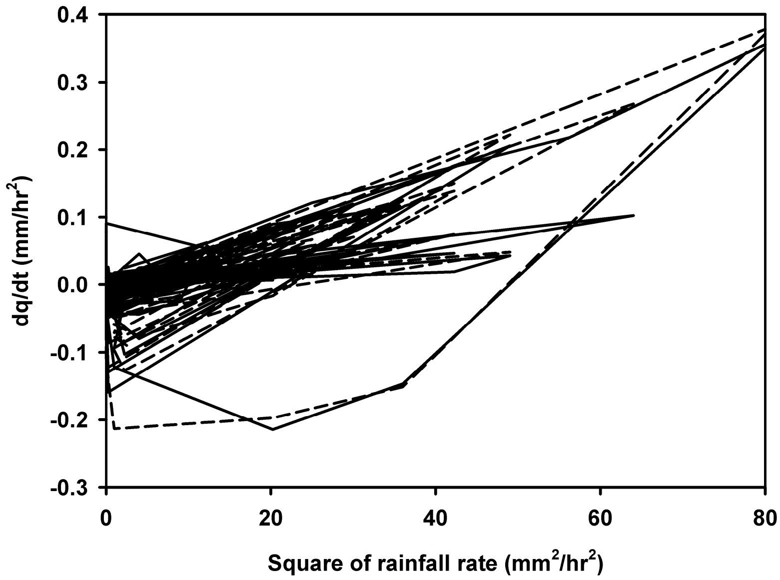

Figure 5 Observed (solid lines) and simulated (dashed lines) rapid discharge transients for 13th December 1989 to 4th March 1990, inclusive.

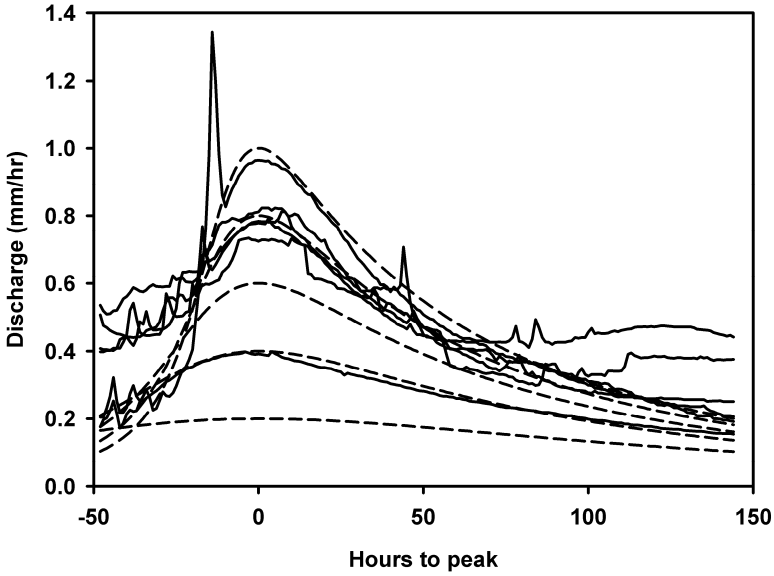

Figure 6 Observed delayed hydrographs (solid lines), and signature hydrographs (dashed lines) for peak discharges of 0.2, 0.4, 0.6, 0.8 and 1.0 mm hr^{-1}.

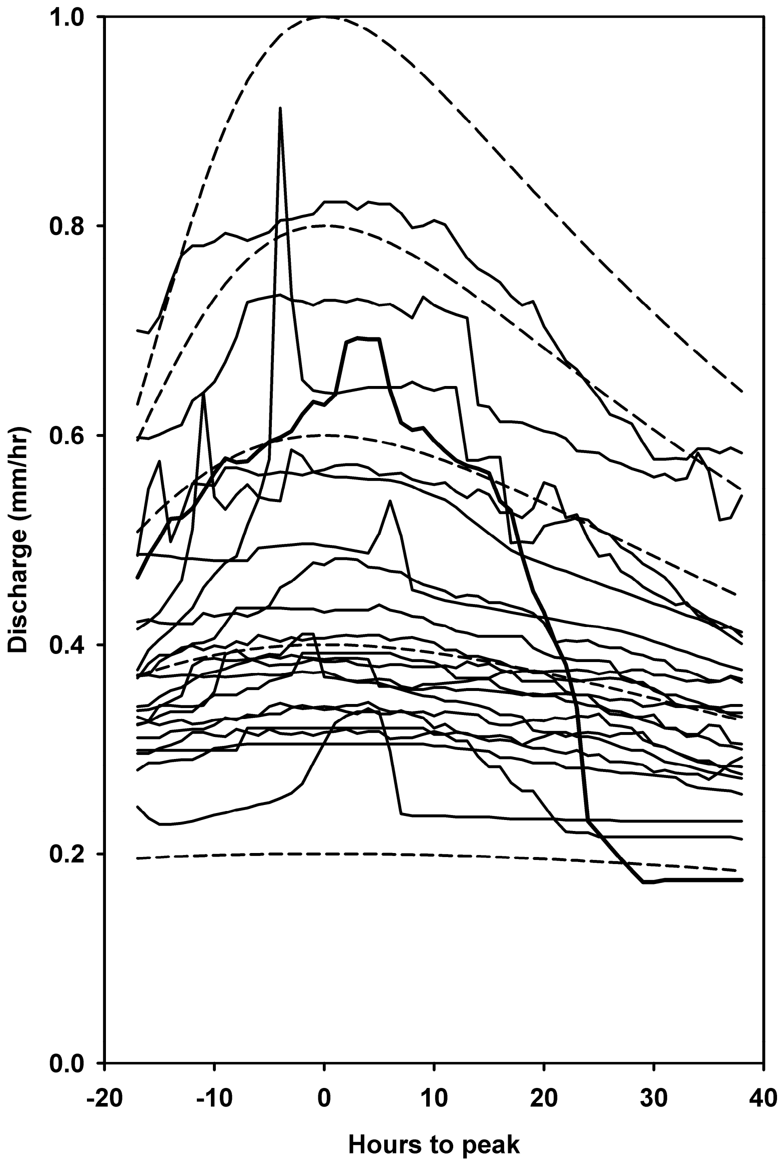

Figure 7 Automatically selected delayed hydrographs for 1971-80 (solid lines), and signature hydrographs (dashed lines) for peak discharges of 0.2, 0.4, 0.6, 0.8 and 1.0 mm hr^{-1}.

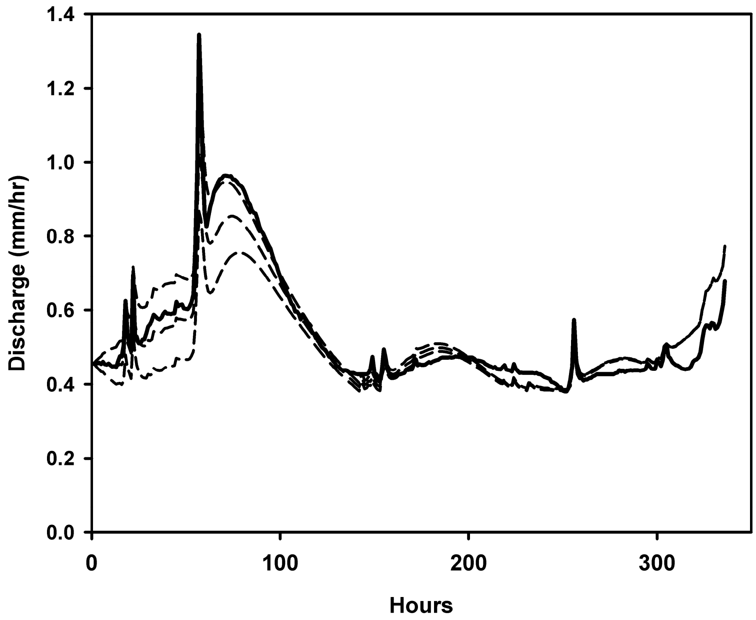

Figure 8 Largest observed delayed hydrograph (solid line) for winter 1989-90, and simulated hydrographs (dashed lines) for initial storages of 60.02, 70.02 and 80.02 mm.

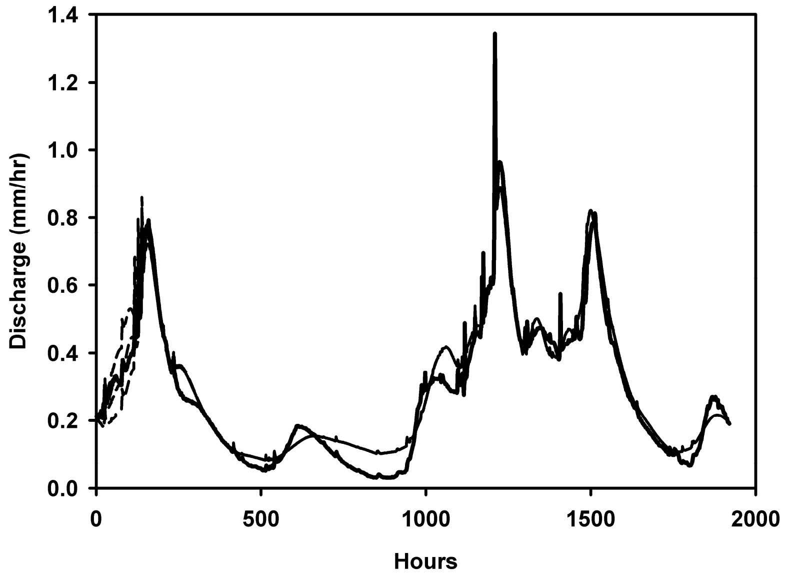

Figure 9 Observed hydrograph (solid line) for winter 1989-90, and simulated hydrographs (dashed lines) for initial storages of 37.22, 47.22, and 57.22 mm.

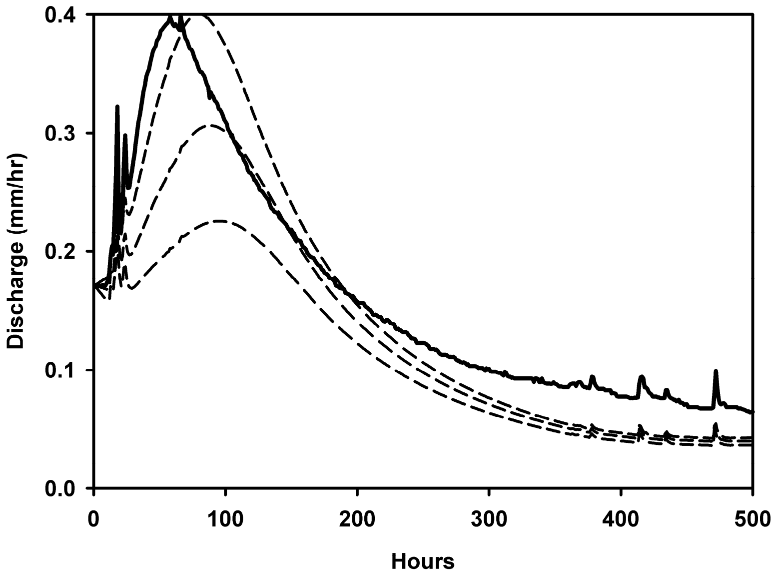

Figure 10 Largest observed delayed hydrograph (solid line) for winter 1990-91, and simulated hydrographs (dashed lines) for initial storages of 32.50, 42.50 and 52.50 mm.

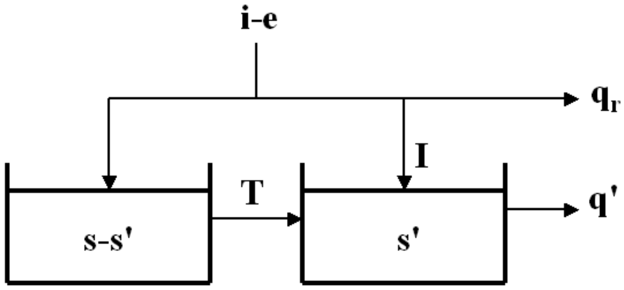

Figure 11 Conventional two-store lumped model.